Radar Reflectivity–Derived Thunderstorm Parameters Applied to Storm Longevity Forecasting

P. L. MACKEEN,* H. E. BROOKS, AND K. L. ELMORE*

NOAA/Environmental Research Labs, National Severe Storms Laboratory, Norman, Oklahoma

22 May 1998 and 2 November 1998

ABSTRACT

In order for the Federal Aviation Administration (FAA) to use airspace more efficiently during thunderstorm events, accurate storm longevity forecasts are needed. Relationships between 16 radar reflectivity–derived storm characteristics and storm longevity are examined to determine which, if any, of the storm characteristics are strongly related to storm lifetime. Such relationships are potentially useful for the development of storm longevity forecasts. The study includes 879 storms that formed over the Memphis, Tennessee, area during 15 late spring and summer convective days. Statistical analyses comparing all 16 storm characteristics to the observed remaining lifetime show that these storm characteristics are not good predictors for storm remaining lifetime.

1. Introduction

In the warm season, major air traffic delays often are caused by convective weather. Although this seems straightforward, impacts on airport capacity by small areas of convective weather can be profound. These impacts are discussed herein as they apply to terminal areas within the United States. Impacts on airport capacity occur primarily because arriving flight paths are more confined than departing flight paths; airport capacity is more limited by the ability to accept arrivals than by the ability to discharge departures. At major airports, arriving flights are constrained to fly over a point in space, or within a narrow corridor around that point, called an arrival gate. In addition, these points must be traversed at specific altitudes. Major airports typically maintain four arrival gates, located roughly 60 km to the northeast, northwest, southwest, and southeast of the airport; departures are discharged in the cardinal directions. To maintain proper spatial separation between arriving aircraft, all pass through the arrival gate in single file at specified intervals. At peak demand times, aircraft are expected to be able to pass through all four arrival gates using minimal separation; any peak capacity reduction by either lost access to an arrival gate or by an increase in interval spacing results in delays. Since safety considerations prevent jet transport aircraft from penetrating active convection, convection near or around an arrival gate causes that gate to become unavailable.

Currently, air traffic control (ATC) responses to convective weather are reactive: either holding distant departing flights until the weather is no longer effecting the arrival gate or diverting flights to other, unaffected arrival gates, causing in-flight holds. Because in-flight holds are expensive for air carriers and quickly fill up available airspace with holding aircraft, they are avoided whenever possible. For aircraft already en route, flight mileage (and fuel burn) may increase as they are redirected to available gates. At worst, en route flights are forced to divert to alternate destinations at high cost to air carriers and passengers.

Holding departing flights often leads to inefficient airspace use because ATC has no reliable product that forecasts when adverse weather will dissipate or exit affected gates, making them available again. As such, ATC holds flights at distant departure points until the weather has moved out or dissipated, which means that there are significant periods of available capacity that cannot be utilized since no flights are en route (Evans 1997). Clearly, in order to use airspace more efficiently during thunderstorm events, accurate storm longevity forecasts are needed. Evans (1997) estimated spatial and temporal accuracy required of convective weather forecasts. He found that lead times as short as 20–30 min would be operationally useful within about 74 km of the airport in a region referred to as the airport terminal area (ATA). Location errors in the ATA must be within 5–10 km, whereas location errors within about 10 km

* Additional affiliation: University of Oklahoma, Cooperative Institute for Mesoscale Meteorological Studies, Norman, Oklahoma.

Corresponding author address: Pamela L. MacKeen, National Severe Storms Laboratory, 1313 Halley Circle, Norman, OK 73069.
E-mail: mackeen@nssl.noaa.gov

of the runways require 5–10-min temporal and 2-km spatial accuracy. A convective forecasting product development team (PDT), composed of scientists from Lincoln Laboratory, the National Center for Atmospheric Research (NCAR), and the National Severe Storms Laboratory (NSSL), is collaborating to develop techniques for thunderstorm initiation, growth, and decay forecasting that will meet the needs of the Federal Aviation Administration (FAA) as part of the Integrated Terminal Weather System (ITWS) development (Wolfson et al. 1997). This paper reports part of NSSL's findings related to this effort.

In this paper we analyze the utility of radar reflectivity–derived (Table 2) characteristics as predictors of storm remaining lifetime. We investigated single- and multicelled storms that did not develop into well-organized convection. Since this study was designed to examine predictors for convective events characterized by timescales on the order of tens of minutes to a few hours, organized convective events with longer timescales (e.g., squall lines) were excluded. Also, since there are no appropriate automated velocity products applicable to nonsupercell storms in the current National Weather Service (NWS) operational suite of radar-based algorithms, none were used.

A number of previous radar-based convective longevity studies examined relationships between storm longevity and storm characteristics such as size, intensity, and top height. For example, Battan (1953) showed that for single-celled storms, storm duration increased with increased storm horizontal extent for storms with horizontal diameters less than 3 mi. Battan (1952) also found that the storm-top heights associated with ''longer lived'' (20 min) single-cell convection were higher than those associated with shorter-lived (~10 min) cells.

Whereas Battan's studies investigated relationships between storm duration and individual storm characteristics, more recent studies (including the current study) have investigated relationships between storm duration and multiple storm characteristics. For instance, Henry (1993) analyzed the relationship between storm duration and both storm size, measured by volume, and maximum reflectivity. The goal of Henry's study was very similar to the goal of this study, but the data were somewhat different. In Henry's study, storms were defined by a single reflectivity threshold, 35 dBZ_e, and a minimum volume of 50 km^3, using the Thunderstorm Identification, Tracking, Analysis, and Nowcasting (TITAN) algorithm (Dixon and Wiener 1993). Single and multicelled storms were analyzed separately and storm characteristics were sampled every 30 min. Like the current study, Henry's omitted supercells. The study showed that storms with volumes greater than 400 km^3 and maximum reflectivities of 53 dBZ_e or greater had a mean remaining lifetime of 30 min or more. Also, simple (single celled) storms had a much greater probability of dissipating (83%) within 30 min than complex (merging) storms (12%).

The relation of storm size and intensity to storm duration was also analyzed by Wilson (1966). Wilson addressed the predictability of convection by determining how far into the future various convective scales and intensities were likely to persist. In this study, Wilson determined scale and intensity predictability by cross correlating echo patterns (5–40-mi wavelength) over several time intervals (5–180 min). Results showed that forecast timescale decreased with decreasing echo scale, but increased with increasing echo intensity (reflectivity). However, cross correlations between reflectivity patterns of different scale were quite variable; in some cases the same forecast timescale appeared valid for different echo scales. Therefore, Wilson did not specify a general set of rules for predicting echo longevity based on echo scale.

Others have addressed the relationship between the scale of weather disturbances, their duration, and predictability. These studies are important to the current work because they provide guidance for defining both the convective scale that falls within a radar's domain and the time period over which the convective scale's duration may be forecast. Based on Orlanski's (1975) scale definitions, convective scales that fall within the radar domain used in this work (125 km) include thunderstorms, cloud clusters, and squall lines (scales 2–200 km), with durations from 30 min to a day. These convective scales have typical time periods of valid linear extrapolation which were estimated by Zipser (1983). For instance, estimated valid linear extrapolation timescale for an individual thunderstorm was 5–20 minutes, a severe thunderstorm 10 min–1 h, and thunderstorms organized on the mesoscale (e.g., squall lines, complexes) about 1–2 h. The current study addresses whether reflectivity-derived characteristics (Table 2) associated with individual, nonrotating thunderstorms can provide a convective duration forecast on the order of 30 min, a forecast timescale invalid for forecasts based on extrapolation alone.

In addition to the storm characteristics discussed previously, clear-air signatures, such as outflow boundaries and other zones of localized convergence, have been applied to storm longevity forecasting. Detection of these clear-air signatures can aid forecasting by highlighting zones of enhanced lift that may help initiate or sustain convection. For example, Wilson and Megenhardt (1997) showed that storms tend to be longer lived when boundary-relative storm motion is approximately zero. Although convergence boundaries can be useful in storm longevity forecasts, their application is limited. For instance, boundaries are only detectable close to the radar (~50 km) and are limited by terrain blockage in mountainous areas. Furthermore, not all convergence boundaries are associated with new convection. Stensrud and Maddox (1988) exemplified this scenario through an analysis of colliding mesoscale outflows from two mesoscale convective systems that moved into an area of potential instability without producing additional convection. They concluded that the anvils associated with the two mesoscale convective systems collided at approximately the same time as the outflows, producing an opposing downward circulation that impeded convective initiation. In this case, the ability to forecast convective initiation was limited by available observations.

Within the last decade, results from the above and other related studies have been used to develop algorithms that forecast storm initiation, growth, and decay. For instance, Wolfson et al. (1994) developed the ITWS Microburst Prediction Algorithm using machine-intelligent image processing and data-fusion techniques to detect regions of storm growth and decay. The feasibility of using components of this algorithm to make short-term convective forecasts for the FAA is currently under investigation. NCAR scientists are also working toward short-term forecasts for the FAA. They continue to develop the Auto-nowcaster (Wilson et al. 1997), an automated system that utilizes radar, satellite, and surface and upper-air weather observations to make 0–60-min forecasts of thunderstorm initiation, movement, and dissipation. In the United Kingdom, Hand and Conway (1995) developed a rule-based model for convection that used radar-estimated rainfall rates and cloud-top temperatures to forecast the convective stage of a storm on 30-min intervals out to 3 h. For a more thorough review of the history and the status of short-term convective precipitation forecasts, see Wilson et al. (1997).

For this study, we analyzed the statistical relationships between 16 radar reflectivity–derived characteristics and observed remaining storm lifetime for our sample. The study was based on radar reflectivity–derived characteristics that estimate storm height, size, and intensity. These characteristics were analyzed to determine not only their general relationships with storm remaining lifetime, but their practical value for storm longevity prediction. This paper will show that simple treatment of these reflectivity-derived parameters offers limited value for storm longevity prediction.

2. Data and method

In this study, reflectivity-derived parameters were determined using Weather Surveillance Radar-1988 Doppler (WSR-88D) level II archived data that were collected using Volume Coverage Pattern (VCP) 21,[1] for 15 days during the 1995–96 late spring and summer seasons in Memphis, Tennessee (Table 1). Although radar data collected in VCP 11 would have been ideal for this study, most of the available data had been collected using VCP 21. Therefore, to avoid mixing data from two different VCPs, we limited the dataset only to that collected using VCP 21. In addition, the data were limited to the Memphis area because Memphis was an FAA ITWS test bed during 1996 and the Convective Weather PDT's efforts were focused on examining these data.

[1] The VCP 21 (11) mode utilizes 9 (14) elevation slices from 0.5° to 19.5° and a new start to the volume scan approximately every 6 (5) min.

TABLE 1. Dates and time periods of WSR-88D data and the CAPE and BRNSHR (Nashville–Jackson) determined from the most recent 0000 UTC sounding for each day; M denotes missing data.

Date	Time period (UTC)	CAPE (J kg^{-1})	BRNSHR (m s^{-1})
06 Jun 1995	1615–1847 1947–2202	5/1042	0/36
14 Jul 1995	1904–2345	M	M
17 Jun 1995	2010–2330	88/12	10/0.12
17 Aug 1995	1723–0105	2765/2363	0.18/6.88
19 Aug 1995	1946–0102	3329/1753	6.97/0.51
13 Jun 1996	1520–2122	1411/444	6.35/21.14
22 Jun 1996	1917–2315	1218/M	11.6/M
23 Jun 1996	2145–0020	0.0/1950	0.0/1.48
29 Jun 1996	1818–0020	11/M	0.47/M
08 Jul 1996	1926–1008	43/1935	43/25.12
16 Jul 1996	1857–0241	0.0/340	0.0/0.68
08 Aug 1996	1639–0516	522/467	18.64/2.28
12 Aug 1996	1700–0042	620/278	2.42/21.38
17 Aug 1996	1805–0105	766/162	8.41/7.71
30 Aug 1996	1642–0023	214/3.0	3.68/3.0

Soundings are not routinely taken at Memphis. Therefore, to provide insight into the environmental conditions within the Memphis radar domain for each day, the convective available potential energy (CAPE) and the bulk Richardson number shear (BRNSHR) were determined for the most recent 0000 UTC soundings from the two closest sounding sites, Jackson, Mississippi, and Nashville, Tennessee (Table 1). The calculation of CAPE was based on lifting a well-mixed parcel from the lowest 500 m (mean temperature and mixing ratio), and the BRNSHR is simply the denominator of the bulk Richardson number (BRN), defined originally by Moncreiff and Green (1972) as

$$\mathrm{BRN} = \frac{\mathrm{CAPE}}{0.5(\overline{u}^2 + \overline{v}^2)}, \quad (1)$$

where $\overline{u}$ and $\overline{v}$ are the wind components of the difference between the density-weighted mean winds over the lowest 6000 m and the lowest 500 m above ground level. Based on these soundings, the environments associated with the examined storms likely contained low-to-moderate BRNSHR (Stensrud et al. 1997) but a wide range in CAPE.

For each day, the WSR-88D reflectivity data were run through the Storm Cell Identification and Tracking (SCIT) algorithm (Johnson et al. 1998) and the Hail Detection Algorithm (HDA; Witt et al. 1998). The SCIT algorithm identified the storms, calculated storm characteristics (Table 2), and tracked storm movement. Johnson et al. (1998) described explicitly the storm identification and tracking process. The HDA predicted the probability of hail of any size, the probability of severe hail (as defined by the NWS), and maximum expected

TABLE 2. Radar-derived storm characteristics from the SCIT and HDA algorithms and their units.

Characteristic	Units
Max reflectivity	dBZ_e
Cell-based vertically integrated liquid	kg m^{-2}
Volume	km^3
Mass	kg $\times$ 10^6
Area	km^2
Storm-top height	km
Storm-base height	km
Top height of 40-dBZ_e core	km
Base height of 40-dBZ_e core	km
Probability of hail	%
Probability of severe hail	%
Maximum hail size	in.
Maximum reflectivity height	km
Center of mass height	km
Core aspect ratio (ratio of storm core depth to its width)	ratio
Reflectivity ratio (ratio of maximum reflectivity to reflectivity at the lowest elevation angle)	ratio

TABLE 3. Remaining lifetime and storm characteristic product-moment correlation coefficients at the 99% confidence level.

Characteristic	Pearson's r
Max reflectivity	0.36
Height of max reflectivity	0.34
Center of mass height	0.33
Top height of 40-dBZ_e core	0.33
Cell-based VIL	0.33
Storm-top height	0.32
Core aspect ratio	0.29
Mass	0.27
Hail probability	0.25
Reflectivity ratio	0.23
Area	0.17
Volume	0.16
Base height of 40-dBZ_e core	0.13
Storm-base height	0.05
Max hail size	−0.01
Severe hail probability	−0.01

hail size associated with each storm. Both the SCIT algorithm and the HDA were developed to provide information about storm state and severity, and are analyzed here to determine their value in statistical storm longevity forecasting.

Once the storms were identified by the (SCIT) algorithm, a radar meteorologist manually verified the storm tracks. In order to manually verify the storm tracks, NSSL's Radar Analysis and Detection System (Sanger et al. 1995) was used to display both the raw reflectivity data and the algorithm-derived storm tracks. Storm tracks were verified to ensure that only accurate storm lifetimes were included in the dataset. Next, storms were selected that met the following criteria for the study's dataset: 1) lifetime greater than or equal to 12 min, 2) maximum reflectivity 40 dBZ_e or greater, and 3) storm track within 30–125 km of the radar. These criteria were chosen to address FAA needs. For instance, the 40-dBZ_e maximum reflectivity threshold was selected to define storm lifetime because pilots tend to avoid convective areas containing reflectivity greater than or equal 40 dBZ_e (Evans 1997). The range domain was chosen to 1) include airspace that has greatly affected airport capacity and 2) minimize radar sampling errors. Finally, reflectivity-based characteristic time series were created for each storm. Table 2 lists the 16 SCIT storm characteristics used in this study. Upon completion of this process, the dataset contained 879 storms and their 16 storm characteristic trends.

Statistical relationships between the 16 storm characteristic trends and storm remaining lifetime were derived using linear univariate and multiple regression analysis. For the linear univariate analysis, the magnitude of each storm characteristic for each volume scan (every 6 min) throughout its lifetime was correlated with its remaining lifetime. This analysis was also completed using the magnitude of a storm characteristic every other and every third volume scan within a trend. However, this analysis failed to provide any added benefit. Remaining lifetime was calculated by subtracting the current storm duration from the total storm lifetime for each volume scan in a storm characteristic time series. Also, remaining lifetime probability density functions (pdfs) were determined for each storm characteristic. For the linear multivariate analysis, the magnitudes of all the storm characteristics were correlated with remaining lifetime.

In addition to analyzing the relationship between storm characteristic magnitude and remaining lifetime, it was determined whether storm characteristic magnitude, in conjunction with a simple measure of storm growth or decay, strengthened any relationship with remaining lifetime. Storm growth or decay was measured by calculating storm characteristic differences over one, two, and three consecutive volume scans.

3. Results

Analysis methods showed that none of the storm characteristics used in this study were good predictors for remaining storm lifetime. For example, both the univariate and multivariate statistical analyses measured weak to moderately weak linear relationships between radar-derived storm characteristics and remaining lifetime. Individually, the strongest relationships [Pearson's linear product moment correlation coefficient (r) greater than 0.3] were between variables that estimate storm intensity and height (Table 3). Remaining lifetime was correlated slightly better with combinations of storm characteristics than with any single characteristic. Combining all 16 characteristics, multiple linear regression

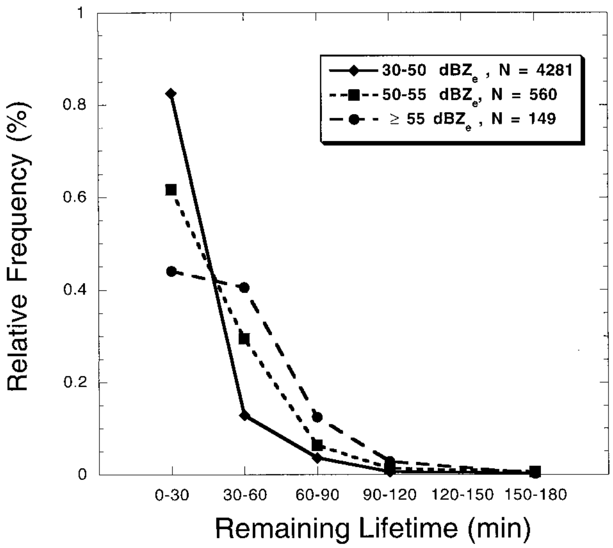

FIG. 1. Remaining lifetime probability distribution functions for three maximum reflectivity categories (30–50, 50–55, and ≥55 dBZ_e); *N* is the number of elements in each distribution.

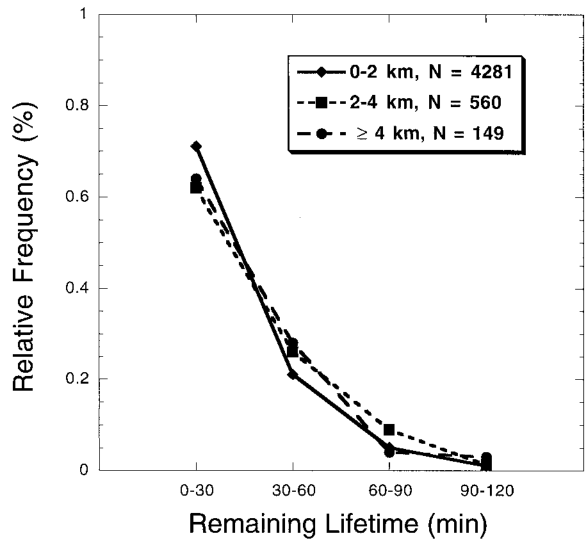

FIG. 2. Remaining lifetime probability distribution functions for three base-height categories (0–2, 2–4, and ≥4 km); *N* is the number of elements in each distribution.

analysis provided a multiple linear coefficient of r = 0.43.

To understand the relationship between these storm characteristics and remaining lifetime better, a discrete pdf of remaining lifetime was constructed for each variable. Since maximum reflectivity was most strongly correlated with remaining lifetime, maximum reflectivity-based pdf's were used to illustrate the best example of storm characteristic time series as a potential predictor of storm longevity (Fig. 1). These probability distributions are interpreted as the probability of a storm having a certain remaining lifetime range, given a maximum reflectivity value within one of the three maximum reflectivity categories. For example, storms with a maximum reflectivity value between 30 and 50 dBZ_e had the greatest probability (82%) of dissipating within 30 min, whereas storms with a maximum reflectivity greater than 55 dBZ_e had only a 44% probability of dissipating within 30 min. In contrast, the pdf associated with storm-base height (see Fig. 2), which was essentially uncorrelated with remaining lifetime, showed that base height fails to discriminate remaining lifetime.

The remaining lifetime pdf's associated with storm trends and storm characteristic magnitude were similar to those associated only with storm magnitude. Examples of these pdf's are shown in Fig. 3. Comparison between Figs. 3a and 3b shows that storms with mass less than or equal to 100×10^6 were more likely to dissipate within 30 min than storms with mass greater than or equal to 200×10^6 kg. Also, regardless of mass magnitude, ''dissipating'' storms were more likely to die within 30 min than growing storms. However, adding a simple growth and decay measure to the dataset did not significantly improve storm remaining lifetime discrimination.

4. Discussion

The general, qualitative relationships between storm duration and measures of storm intensity, height, and size were similar to those determined by previous authors; namely storm remaining lifetime increased with increasing storm-top height, size, and intensity. However, the purpose of this study was to determine the practical application of storm characteristics in forecasts of storm remaining lifetime. In contrast to Henry's (1993) study, storms were defined by SCIT using seven reflectivity thresholds, single- and multicelled storms were analyzed jointly, and storms were sampled every volume scan (6 min). As a result of storm definition differences, Henry's study calculated echo volume within a 35-dBZ_e contour, whereas this study calculates only the storm core volume (Johnson et al. 1998). The correlation coefficients calculated by Henry for both volume and maximum reflectivity with respect to remaining storm lifetime ranged from 0.39 to 0.52. Henry's correlation coefficients are somewhat larger than those found in this study, most likely owing to computing storm characteristics based on a larger storm echo. However, both studies show that relationships between storm characteristics and remaining lifetime are not large enough to discriminate between short- and long-lived storms.

Owing to the large size of the dataset, all correlation coefficients are statistically significant at the 99% confidence level. However, not all statistically significant results have *practical* significance from an operational perspective. In the univariate portion of this study, maximum reflectivity and remaining lifetime share the greatest coefficient of determination (r^2 = 0.13). This means that only 13% of the variance in remaining lifetime is

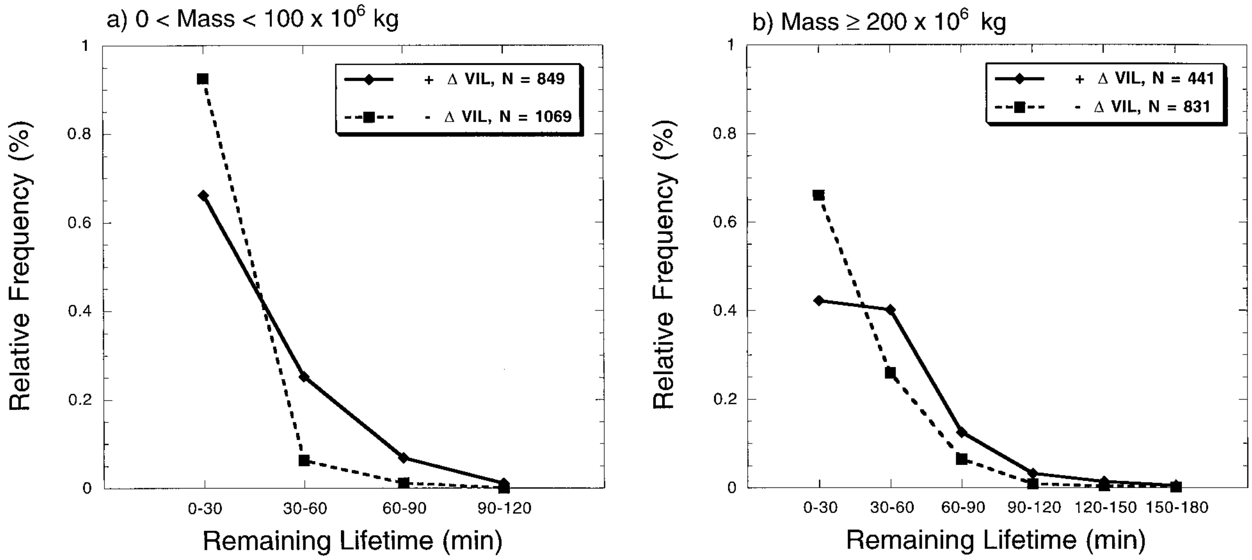

FIG. 3. Remaining lifetime probability distribution functions for positive (solid line) and negative (dashed line) changes in cell-based vertically integrated liquid (VIL) time series and storm mass (a) greater than 0 but less than 100×10^6 kg and (b) greater than or equal to 200×10^6 kg; N is the number of elements in each distribution. Cell-based VIL differences are denoted by ΔVIL; the plus (negative) sign represents growth (dissipation).

explained by maximum reflectivity. The percentage of remaining lifetime variance explained by the multivariate storm characteristics analysis is slightly greater ($r^2 = 0.18$). In this light, these weak relationships make using this study's storm characteristics as storm longevity predictors questionable at best, especially compared to the forecast criteria noted by Evans (1997).

Given these results, a natural question is why radar reflectivity–derived storm characteristic measurements, and especially their trends, are so poorly related to remaining lifetime. There are several possible answers to this question. Since convective processes are nonlinear, linear relationships between storm characteristics and storm longevity necessarily will be limited. In addition, relationships between these variables are also limited by the WSR-88D's and algorithms' ability to observe, detect, and characterize storms. Inherent radar sampling problems such as ground clutter contamination and anomalous propagation all affect the final reflectivity fields ingested by storm detection algorithms. Including these reflectivity features within an algorithm-defined storm results in false detections.

Other radar sampling limitations like beam spreading and range-dependent beam height can result in incorrect storm characteristic measurements, and especially their trends. As a result, variations in the characteristics we calculate can be due to either actual changes in storm state or variations in radar sampling. Howard et al. (1997) addressed this problem by showing that the WSR-88D's inherent uncertainties (owing especially to radar range and the VCP) resulted in uncertainty in reflectivity-derived trends. Based on this result, Howard et al. strongly suggested that the uncertainty associated with storm-based parameters (e.g., storm-top height, height of maximum reflectivity, etc.) needs to be considered, especially when trying to develop relationships between thunderstorm characteristics and rate of growth and decay. Whether consideration of height uncertainty can improve the relationship between storm height parameters and storm growth and decay is yet to be determined.

Two additional points to keep in mind are that 1) the WSR-88D reflectivity is a measure of the scattering from hydrometeors produced by convection rather than the convective process itself, and 2) reflectivity data are the result of convective processes temporally integrated over an indeterminate time frame. Also, different storms may not enjoy parallel evolution, which precludes the use of a single analysis method to capture storm characteristic and remaining lifetime relationships to their fullest extent.

Although it is likely that radar reflectivity–derived storm characteristics fail to represent adequately the convective processes that are needed for use in statistical forecasts of storm longevity, reflectivity-derived characteristics combined with other data sources may discriminate storm longevity better; especially for more organized convection. For example, trends of velocity-derived characteristics associated with mesocyclones such as maximum strength, depth, and midlevel versus low-level base may be correlated better with remaining storm duration. Work addressing the use of both velocity and reflectivity-derived characteristics associated with mesocyclones is currently under way and will be reported subsequently. Additionally, environmental conditions measured by in situ, satellite, and other data sources, or predicted by a model, could provide information concerning the environment's ability to support convection, or a specific type of convection. One example of this type of analysis is examining mesoscale model forecasts of the environment ahead of an organized convective system, such as a squall line, to determine the forecasts' relationship to the life cycle of the system. Cloud model results, combined with both reflectivity and velocity radar observations also should be investigated for their potential utility as storm duration guidance. For instance, convective evolution forecasts could be provided from numerically simulated storm types and life stages shown to match the storm structure (based on both reflectivity and velocity data) identified on radar.

Acknowledgments. This research was completed in response to requirements and fundings by the Federal Aviation Administration. The views expressed are those of the authors and do not necessarily represent the official policy or position of the FAA. We thank MIT/Lincoln Laboratory for supplying the radar data and Dr. John Cortinas for providing ASCII-conversion programs to expedite the sounding analysis. We also thank a number of our colleagues for their comments and suggestions. In particular, we thank Dr. Rodger Brown, Ken Howard, Dr. Bob Maddox, Barbara Brown, Mike Eilts, and the Convective Weather Product Development Team. In addition, we thank Dr. C. A. Doswell and the two anonymous reviewers for their reviews of the manuscript, which led to numerous improvements. Thanks also to Mike Francis for his contribution to the storm tracking verification.

REFERENCES

Battan, L. J., 1952: Formation of precipitation in natural clouds indicated by radar. Preprints, *Third Conference on Radar Meteorology,* Montreal, PQ, Canada, Amer. Meteor. Soc., A9–A16.

——, 1953: Duration of convective radar cloud units. *Bull. Amer. Meteor. Soc.,* **34,** 227–228.

Dixon, M., and G. Wiener, 1993: TITAN: Thunderstorm Identification, Tracking, Analysis, and Nowcasting—A radar-based methodology. *J. Atmos. Oceanic Technol.,* **10,** 785–979.

Evans, J. E., 1997: Operational problem of convective weather in the national airspace system. Preprints, *Convective Weather Forecasting Workshop,* Long Beach, CA, A1–A14.

Hand, W. H., and B. J. Conway, 1995: An object-oriented approach to nowcasting showers. *Wea. Forecasting,* **10,** 327–341.

Henry, S. G., 1993: Analysis of thunderstorm lifetime as a function of size and intensity. Preprints, *26th Conf. on Radar Meteorology,* Norman, OK, Amer. Meteor. Soc., 138–140.

Howard, K. W., J. J. Gourley, and R. A. Maddox, 1997: Uncertainties in WSR-88D measurements and their impacts on monitoring life cycles. *Wea. Forecasting,* **12,** 166–174.

Johnson, J. T., P. L. MacKeen, A. E. Witt, E. D. Mitchell, G. J. Stumpf, M. D. Eilts, and K. W. Thomas, 1998: The storm cell identification and tracking algorithm: An enhanced WSR-88D algorithm. *Wea. Forecasting,* **13,** 263–276.

Moncrieff, M. W., and J. S. A. Green, 1972: The propagation and transfer properties of steady convective overturning in shear. *Quart. J. Roy. Meteor. Soc.,* **98,** 336–352.

Orlanski, I., 1975: A rational subdivision of scales for atmospheric processes. *Bull. Amer. Meteor. Soc.,* **56,** 527–530.

Sanger, S. S., R. M. Steadham, J. M. Jarboe, R. E. Schlegel, and A. Sellakannnu, 1995: Human factors contributions to the evolution of an interactive Doppler radar and weather detection algorithm display system. Preprints, *11th Int. Conf. on Interactive Information and Processing Systems for Meteorology, Oceanography, and Hydrology,* Dallas, TX, Amer. Meteor. Soc., 1–6.

Stensrud, D. J., and R. A. Maddox, 1988: Opposing mesoscale circulations: A case study. *Wea. Forecasting,* **3,** 189–204.

——, J. V. Cortinas Jr., and H. E. Brooks, 1997: Discriminating between tornadic and nontornadic thunderstorms using mesoscale model output. *Wea. Forecasting,* **12,** 613–632.

Wilson, J. W., 1966: Movement and predictability of radar echoes. Tech. Memo IERTM-NSSL-28, National Severe Storms Laboratory, 30 pp. [Available from National Information Service, Operations Division, Springfield, VA 22161.]

——, and D. L. Megenhardt, 1997: Thunderstorm initiation, organization, and lifetime associated with Florida boundary layer convergence lines. *Mon. Wea. Rev.,* **125,** 1507–1525.

——, A. Crook, C. Mueller, and M. Dixon, 1997: State-of-the-art of nowcasting thunderstorms. Preprints, *Convective Weather Forecasting Workshop,* Long Beach, CA, B1–B38.

Witt, A., M. D. Eilts, G. J. Stumpf, J. T. Johnson, E. D. Mitchell, and K. W. Thomas, 1998: An enhanced hail detection algorithm for the WSR-88D. *Wea. Forecasting,* **13,** 286–303.

Wolfson, M. M., F. L. Delanoy, B. E. Forman, F. G. Hallowell, M. L. Pawlak, and P. D. Smith, 1994: Automated microburst windshear prediction. *Lincoln Lab. J.,* **7,** 399–426.

——, C. K. Mueller, and M. Eilts, 1997: Convective weather forecasting for FAA applications. Preprints, *Seventh Conf. on Aviation, Range, and Aerospace Meteorology,* Long Beach, CA, Amer. Meteor. Soc., 238–243.

Zipser, E. J., 1983: Nowcasting and very-short-range forecasting. *The National STORM Program: Scientific and Technical Bases and Major Objectives,* University Corporation for Atmospheric Research, 6–1 to 6–30.